FERMILAB-PUB-XX-XXX-X

Measurement of the Forward-Backward Asymmetry in the $B \to K^{(*)}\mu^+\mu^-$ Decay and First Observation of the $B_s^0 \to \phi\mu^+\mu^-$ Decay

T. Aaltonen,[22] B. Álvarez González[v],[10] S. Amerio,[42] D. Amidei,[33] A. Anastassov,[37] A. Annovi,[18] J. Antos,[13] G. Apollinari,[16] J.A. Appel,[16] A. Apresyan,[47] T. Arisawa,[56] A. Artikov,[14] J. Asaadi,[52] W. Ashmanskas,[16] B. Auerbach,[59] A. Aurisano,[52] F. Azfar,[41] W. Badgett,[16] A. Barbaro-Galtieri,[27] V.E. Barnes,[47] B.A. Barnett,[24] P. Barria[ee],[45] P. Bartos,[13] M. Bauce[cc],[42] G. Bauer,[31] F. Bedeschi,[45] D. Beecher,[29] S. Behari,[24] G. Bellettini[dd],[45] J. Bellinger,[58] D. Benjamin,[15] A. Beretvas,[16] A. Bhatti,[49] M. Binkley*,[16] D. Bisello[cc],[42] I. Bizjak[ii],[29] K.R. Bland,[5] C. Blocker,[7] B. Blumenfeld,[24] A. Bocci,[15] A. Bodek,[48] D. Bortoletto,[47] J. Boudreau,[46] A. Boveia,[12] B. Brau[a],[16] L. Brigliadori[bb],[6] A. Brisuda,[13] C. Bromberg,[34] E. Brucken,[22] M. Bucciantonio[dd],[45] J. Budagov,[14] H.S. Budd,[48] S. Budd,[23] K. Burkett,[16] G. Busetto[cc],[42] P. Bussey,[20] A. Buzatu,[32] S. Cabrera[x],[15] C. Calancha,[30] S. Camarda,[4] M. Campanelli,[34] M. Campbell,[33] F. Canelli[12],[16] A. Canepa,[44] B. Carls,[23] D. Carlsmith,[58] R. Carosi,[45] S. Carrillo[k],[17] S. Carron,[16] B. Casal,[10] M. Casarsa,[16] A. Castro[bb],[6] P. Catastini,[16] D. Cauz,[53] V. Cavaliere[ee],[45] M. Cavalli-Sforza,[4] A. Cerri[f],[27] L. Cerrito[q],[29] Y.C. Chen,[1] M. Chertok,[8] G. Chiarelli,[45] G. Chlachidze,[16] F. Chlebana,[16] K. Cho,[26] D. Chokheli,[14] J.P. Chou,[21] W.H. Chung,[58] Y.S. Chung,[48] C.I. Ciobanu,[43] M.A. Ciocci[ee],[45] A. Clark,[19] D. Clark,[7] G. Compostella[cc],[42] M.E. Convery,[16] J. Conway,[8] M.Corbo,[43] M. Cordelli,[18] C.A. Cox,[8] D.J. Cox,[8] F. Crescioli[dd],[45] C. Cuenca Almenar,[59] J. Cuevas[v],[10] R. Culbertson,[16] D. Dagenhart,[16] N. d'Ascenzo[t],[43] M. Datta,[16] P. de Barbaro,[48] S. De Cecco,[50] G. De Lorenzo,[4] M. Dell'Orso[dd],[45] C. Deluca,[4] L. Demortier,[49] J. Deng[c],[15] M. Deninno,[6] F. Devoto,[22] M. d'Errico[cc],[42] A. Di Canto[dd],[45] B. Di Ruzza,[45] J.R. Dittmann,[5] M. D'Onofrio,[28] S. Donati[dd],[45] P. Dong,[16] T. Dorigo,[42] K. Ebina,[56] A. Elagin,[52] A. Eppig,[33] R. Erbacher,[8] D. Errede,[23] S. Errede,[23] N. Ershaidat[aa],[43] R. Eusebi,[52] H.C. Fang,[27] S. Farrington,[41] M. Feindt,[25] J.P. Fernandez,[30] C. Ferrazza[ff],[45] R. Field,[17] G. Flanagan[r],[47] R. Forrest,[8] M.J. Frank,[5] M. Franklin,[21] J.C. Freeman,[16] I. Furic,[17] M. Gallinaro,[49] J. Galyardt,[11] J.E. Garcia,[19] A.F. Garfinkel,[47] P. Garosi[ee],[45] H. Gerberich,[23] E. Gerchtein,[16] S. Giagu[gg],[50] V. Giakoumopoulou,[3] P. Giannetti,[45] K. Gibson,[46] C.M. Ginsburg,[16] N. Giokaris,[3] P. Giromini,[18] M. Giunta,[45] G. Giurgiu,[24] V. Glagolev,[14] D. Glenzinski,[16] M. Gold,[36] D. Goldin,[52] N. Goldschmidt,[17] A. Golossanov,[16] G. Gomez,[10] G. Gomez-Ceballos,[31] M. Goncharov,[31] O. González,[30] I. Gorelov,[36] A.T. Goshaw,[15] K. Goulianos,[49] A. Gresele,[42] S. Grinstein,[4] C. Grosso-Pilcher,[12] R.C. Group,[16] J. Guimaraes da Costa,[21] Z. Gunay-Unalan,[34] C. Haber,[27] S.R. Hahn,[16] E. Halkiadakis,[51] A. Hamaguchi,[40] J.Y. Han,[48] F. Happacher,[18] K. Hara,[54] D. Hare,[51] M. Hare,[55] R.F. Harr,[57] K. Hatakeyama,[5] C. Hays,[41] M. Heck,[25] J. Heinrich,[44] M. Herndon,[58] S. Hewamanage,[5] D. Hidas,[51] A. Hocker,[16] W. Hopkins[g],[16] D. Horn,[25] S. Hou,[1] R.E. Hughes,[38] M. Hurwitz,[12] U. Husemann,[59] N. Hussain,[32] M. Hussein,[34] J. Huston,[34] G. Introzzi,[45] M. Iori[gg],[50] A. Ivanov[o],[8] E. James,[16] D. Jang,[11] B. Jayatilaka,[15] E.J. Jeon,[26] M.K. Jha,[6] S. Jindariani,[16] W. Johnson,[8] M. Jones,[47] K.K. Joo,[26] S.Y. Jun,[11] T.R. Junk,[16] T. Kamon,[52] P.E. Karchin,[57] Y. Kato[n],[40] W. Ketchum,[12] J. Keung,[44] V. Khotilovich,[52] B. Kilminster,[16] D.H. Kim,[26] H.S. Kim,[26] H.W. Kim,[26] J.E. Kim,[26] M.J. Kim,[18] S.B. Kim,[26] S.H. Kim,[54] Y.K. Kim,[12] N. Kimura,[56] S. Klimenko,[17] K. Kondo,[56] D.J. Kong,[26] J. Konigsberg,[17] A. Korytov,[17] A.V. Kotwal,[15] M. Kreps,[25] J. Kroll,[44] D. Krop,[12] N. Krumnack[l],[5] M. Kruse,[15] V. Krutelyov[d],[52] T. Kuhr,[25] M. Kurata,[54] S. Kwang,[12] A.T. Laasanen,[47] S. Lami,[45] S. Lammel,[16] M. Lancaster,[29] R.L. Lander,[8] K. Lannon[u],[38] A. Lath,[51] G. Latino[ee],[45] I. Lazzizzera,[42] T. LeCompte,[2] E. Lee,[52] H.S. Lee,[12] J.S. Lee,[26] S.W. Lee[w],[52] S. Leo[dd],[45] S. Leone,[45] J.D. Lewis,[16] C.-J. Lin,[27] J. Linacre,[41] M. Lindgren,[16] E. Lipeles,[44] A. Lister,[19] D.O. Litvintsev,[16] C. Liu,[46] Q. Liu,[47] T. Liu,[16] S. Lockwitz,[59] N.S. Lockyer,[44] A. Loginov,[59] D. Lucchesi[cc],[42] J. Lueck,[25] P. Lujan,[27] P. Lukens,[16] G. Lungu,[49] J. Lys,[27] R. Lysak,[13] R. Madrak,[16] K. Maeshima,[16] K. Makhoul,[31] P. Maksimovic,[24] S. Malik,[49] G. Manca[b],[28] A. Manousakis-Katsikakis,[3] F. Margaroli,[47] C. Marino,[25] M. Martínez,[4] R. Martínez-Ballarín,[30] P. Mastrandrea,[50] M. Mathis,[24] M.E. Mattson,[57] P. Mazzanti,[6] K.S. McFarland,[48] P. McIntyre,[52] R. McNulty[i],[28] A. Mehta,[28] P. Mehtala,[22] A. Menzione,[45] C. Mesropian,[49] T. Miao,[16] D. Mietlicki,[33] A. Mitra,[1] H. Miyake,[54] S. Moed,[21] N. Moggi,[6] M.N. Mondragon[k],[16] C.S. Moon,[26] R. Moore,[16] M.J. Morello,[16] J. Morlock,[25] P. Movilla Fernandez,[16] A. Mukherjee,[16] Th. Muller,[25] P. Murat,[16] M. Mussini[bb],[6] J. Nachtman[m],[16] Y. Nagai,[54] J. Naganoma,[56] I. Nakano,[39] A. Napier,[55] J. Nett,[58] C. Neu[z],[44] M.S. Neubauer,[23] J. Nielsen[e],[27] L. Nodulman,[2] O. Norniella,[23] E. Nurse,[29] L. Oakes,[41] S.H. Oh,[15] Y.D. Oh,[26] I. Oksuzian,[17] T. Okusawa,[40] R. Orava,[22] L. Ortolan,[4] S. Pagan Griso[cc],[42] C. Pagliarone,[53] E. Palencia[f],[10]

V. Papadimitriou,[16] A.A. Paramonov,[2] J. Patrick,[16] G. Pauletta[hh],[53] M. Paulini,[11] C. Paus,[31] D.E. Pellett,[8] A. Penzo,[53] T.J. Phillips,[15] G. Piacentino,[45] E. Pianori,[44] J. Pilot,[38] K. Pitts,[23] C. Plager,[9] L. Pondrom,[58] K. Potamianos,[47] O. Poukhov*,[14] F. Prokoshin[y],[14] A. Pronko,[16] F. Ptohos[h],[18] E. Pueschel,[11] G. Punzi[dd],[45] J. Pursley,[58] A. Rahaman,[46] V. Ramakrishnan,[58] N. Ranjan,[47] I. Redondo,[30] P. Renton,[41] M. Rescigno,[50] F. Rimondi[bb],[6] L. Ristori[45],[16] A. Robson,[20] T. Rodrigo,[10] T. Rodriguez,[44] E. Rogers,[23] S. Rolli,[55] R. Roser,[16] M. Rossi,[53] F. Ruffini[ee],[45] A. Ruiz,[10] J. Russ,[11] V. Rusu,[16] A. Safonov,[52] W.K. Sakumoto,[48] L. Santi[hh],[53] L. Sartori,[45] K. Sato,[54] V. Saveliev[t],[43] A. Savoy-Navarro,[43] P. Schlabach,[16] A. Schmidt,[25] E.E. Schmidt,[16] M.P. Schmidt*,[59] M. Schmitt,[37] T. Schwarz,[8] L. Scodellaro,[10] A. Scribano[ee],[45] F. Scuri,[45] A. Sedov,[47] S. Seidel,[36] Y. Seiya,[40] A. Semenov,[14] F. Sforza[dd],[45] A. Sfyrla,[23] S.Z. Shalhout,[8] T. Shears,[28] P.F. Shepard,[46] M. Shimojima[s],[54] S. Shiraishi,[12] M. Shochet,[12] I. Shreyber,[35] A. Simonenko,[14] P. Sinervo,[32] A. Sissakian*,[14] K. Sliwa,[55] J.R. Smith,[8] F.D. Snider,[16] A. Soha,[16] S. Somalwar,[51] V. Sorin,[4] P. Squillacioti,[16] M. Stanitzki,[59] R. St. Denis,[20] B. Stelzer,[32] O. Stelzer-Chilton,[32] D. Stentz,[37] J. Strologas,[36] G.L. Strycker,[33] Y. Sudo,[54] A. Sukhanov,[17] I. Suslov,[14] K. Takemasa,[54] Y. Takeuchi,[54] J. Tang,[12] M. Tecchio,[33] P.K. Teng,[1] J. Thom[g],[16] J. Thome,[11] G.A. Thompson,[23] E. Thomson,[44] P. Ttito-Guzmán,[30] S. Tkaczyk,[16] D. Toback,[52] S. Tokar,[13] K. Tollefson,[34] T. Tomura,[54] D. Tonelli,[16] S. Torre,[18] D. Torretta,[16] P. Totaro[hh],[53] M. Trovato[ff],[45] Y. Tu,[44] N. Turini[ee],[45] F. Ukegawa,[54] S. Uozumi,[26] A. Varganov,[33] E. Vataga[ff],[45] F. Vázquez[k],[17] G. Velev,[16] C. Vellidis,[3] M. Vidal,[30] I. Vila,[10] R. Vilar,[10] M. Vogel,[36] G. Volpi[dd],[45] P. Wagner,[44] R.L. Wagner,[16] T. Wakisaka,[40] R. Wallny,[9] S.M. Wang,[1] A. Warburton,[32] D. Waters,[29] M. Weinberger,[52] W.C. Wester III,[16] B. Whitehouse,[55] D. Whiteson[c],[44] A.B. Wicklund,[2] E. Wicklund,[16] S. Wilbur,[12] F. Wick,[25] H.H. Williams,[44] J.S. Wilson,[38] P. Wilson,[16] B.L. Winer,[38] P. Wittich[g],[16] S. Wolbers,[16] H. Wolfe,[38] T. Wright,[33] X. Wu,[19] Z. Wu,[5] K. Yamamoto,[40] J. Yamaoka,[15] T. Yang,[16] U.K. Yang[p],[12] Y.C. Yang,[26] W.-M. Yao,[27] G.P. Yeh,[16] K. Yi[m],[16] J. Yoh,[16] K. Yorita,[56] T. Yoshida[j],[40] G.B. Yu,[15] I. Yu,[26] S.S. Yu,[16] J.C. Yun,[16] A. Zanetti,[53] Y. Zeng,[15] and S. Zucchelli[bb6]

(CDF Collaboration[†])

[1]*Institute of Physics, Academia Sinica, Taipei, Taiwan 11529, Republic of China*
[2]*Argonne National Laboratory, Argonne, Illinois 60439, USA*
[3]*University of Athens, 157 71 Athens, Greece*
[4]*Institut de Fisica d'Altes Energies, Universitat Autonoma de Barcelona, E-08193, Bellaterra (Barcelona), Spain*
[5]*Baylor University, Waco, Texas 76798, USA*
[6]*Istituto Nazionale di Fisica Nucleare Bologna,* [bb]*University of Bologna, I-40127 Bologna, Italy*
[7]*Brandeis University, Waltham, Massachusetts 02254, USA*
[8]*University of California, Davis, Davis, California 95616, USA*
[9]*University of California, Los Angeles, Los Angeles, California 90024, USA*
[10]*Instituto de Fisica de Cantabria, CSIC-University of Cantabria, 39005 Santander, Spain*
[11]*Carnegie Mellon University, Pittsburgh, Pennsylvania 15213, USA*
[12]*Enrico Fermi Institute, University of Chicago, Chicago, Illinois 60637, USA*
[13]*Comenius University, 842 48 Bratislava, Slovakia; Institute of Experimental Physics, 040 01 Kosice, Slovakia*
[14]*Joint Institute for Nuclear Research, RU-141980 Dubna, Russia*
[15]*Duke University, Durham, North Carolina 27708, USA*
[16]*Fermi National Accelerator Laboratory, Batavia, Illinois 60510, USA*
[17]*University of Florida, Gainesville, Florida 32611, USA*
[18]*Laboratori Nazionali di Frascati, Istituto Nazionale di Fisica Nucleare, I-00044 Frascati, Italy*
[19]*University of Geneva, CH-1211 Geneva 4, Switzerland*
[20]*Glasgow University, Glasgow G12 8QQ, United Kingdom*
[21]*Harvard University, Cambridge, Massachusetts 02138, USA*
[22]*Division of High Energy Physics, Department of Physics, University of Helsinki and Helsinki Institute of Physics, FIN-00014, Helsinki, Finland*
[23]*University of Illinois, Urbana, Illinois 61801, USA*
[24]*The Johns Hopkins University, Baltimore, Maryland 21218, USA*
[25]*Institut für Experimentelle Kernphysik, Karlsruhe Institute of Technology, D-76131 Karlsruhe, Germany*
[26]*Center for High Energy Physics: Kyungpook National University, Daegu 702-701, Korea; Seoul National University, Seoul 151-742, Korea; Sungkyunkwan University, Suwon 440-746, Korea; Korea Institute of Science and Technology Information, Daejeon 305-806, Korea; Chonnam National University, Gwangju 500-757, Korea; Chonbuk National University, Jeonju 561-756, Korea*
[27]*Ernest Orlando Lawrence Berkeley National Laboratory, Berkeley, California 94720, USA*
[28]*University of Liverpool, Liverpool L69 7ZE, United Kingdom*
[29]*University College London, London WC1E 6BT, United Kingdom*

[30] Centro de Investigaciones Energeticas Medioambientales y Tecnologicas, E-28040 Madrid, Spain
[31] Massachusetts Institute of Technology, Cambridge, Massachusetts 02139, USA
[32] Institute of Particle Physics: McGill University, Montréal, Québec,
Canada H3A 2T8; Simon Fraser University, Burnaby, British Columbia,
Canada V5A 1S6; University of Toronto, Toronto, Ontario,
Canada M5S 1A7; and TRIUMF, Vancouver, British Columbia, Canada V6T 2A3
[33] University of Michigan, Ann Arbor, Michigan 48109, USA
[34] Michigan State University, East Lansing, Michigan 48824, USA
[35] Institution for Theoretical and Experimental Physics, ITEP, Moscow 117259, Russia
[36] University of New Mexico, Albuquerque, New Mexico 87131, USA
[37] Northwestern University, Evanston, Illinois 60208, USA
[38] The Ohio State University, Columbus, Ohio 43210, USA
[39] Okayama University, Okayama 700-8530, Japan
[40] Osaka City University, Osaka 588, Japan
[41] University of Oxford, Oxford OX1 3RH, United Kingdom
[42] Istituto Nazionale di Fisica Nucleare, Sezione di Padova-Trento, [cc] University of Padova, I-35131 Padova, Italy
[43] LPNHE, Universite Pierre et Marie Curie/IN2P3-CNRS, UMR7585, Paris, F-75252 France
[44] University of Pennsylvania, Philadelphia, Pennsylvania 19104, USA
[45] Istituto Nazionale di Fisica Nucleare Pisa, [dd] University of Pisa,
[ee] University of Siena and [ff] Scuola Normale Superiore, I-56127 Pisa, Italy
[46] University of Pittsburgh, Pittsburgh, Pennsylvania 15260, USA
[47] Purdue University, West Lafayette, Indiana 47907, USA
[48] University of Rochester, Rochester, New York 14627, USA
[49] The Rockefeller University, New York, New York 10065, USA
[50] Istituto Nazionale di Fisica Nucleare, Sezione di Roma 1,
[gg] Sapienza Università di Roma, I-00185 Roma, Italy
[51] Rutgers University, Piscataway, New Jersey 08855, USA
[52] Texas A&M University, College Station, Texas 77843, USA
[53] Istituto Nazionale di Fisica Nucleare Trieste/Udine,
I-34100 Trieste, [hh] University of Trieste/Udine, I-33100 Udine, Italy
[54] University of Tsukuba, Tsukuba, Ibaraki 305, Japan
[55] Tufts University, Medford, Massachusetts 02155, USA
[56] Waseda University, Tokyo 169, Japan
[57] Wayne State University, Detroit, Michigan 48201, USA
[58] University of Wisconsin, Madison, Wisconsin 53706, USA
[59] Yale University, New Haven, Connecticut 06520, USA

We reconstruct the rare decays $B^+ \to K^+\mu^+\mu^-$, $B^0 \to K^*(892)^0\mu^+\mu^-$, and $B_s^0 \to \phi(1020)\mu^+\mu^-$ in a data sample corresponding to 4.4 fb^{-1} collected in $p\bar{p}$ collisions at $\sqrt{s} = 1.96$ TeV by the CDF II detector at the Fermilab Tevatron Collider. Using 120 ± 16 $B^+ \to K^+\mu^+\mu^-$ and 101 ± 12 $B^0 \to K^{*0}\mu^+\mu^-$ decays we report the branching ratios. In addition, we report the measurement of the differential branching ratio and the muon forward-backward asymmetry in the B^+ and B^0 decay modes, and the K^{*0} longitudinal polarization in the B^0 decay mode with respect to the squared dimuon mass. These are consistent with the theoretical prediction from the standard model, and most recent determinations from other experiments and of comparable accuracy. We also report the first observation of the $B_s^0 \to \phi\mu^+\mu^-$ decay and measure its branching ratio $\mathcal{B}(B_s^0 \to \phi\mu^+\mu^-) = [1.44 \pm 0.33 \pm 0.46] \times 10^{-6}$ using 27 ± 6 signal events. This is currently the most rare B_s^0 decay observed.

PACS numbers: 13.25 Hw, 13.20 He

*Deceased
†With visitors from [a]University of Massachusetts Amherst, Amherst, Massachusetts 01003, [b]Istituto Nazionale di Fisica Nucleare, Sezione di Cagliari, 09042 Monserrato (Cagliari), Italy, [c]University of California Irvine, Irvine, CA 92697, [d]University of California Santa Barbara, Santa Barbara, CA 93106 [e]University of California Santa Cruz, Santa Cruz, CA 95064, [f]CERN,CH-1211 Geneva, Switzerland, [g]Cornell University, Ithaca, NY 14853, [h]University of Cyprus, Nicosia CY-1678, Cyprus, [i]University College Dublin, Dublin 4, Ireland, [j]University of Fukui, Fukui City, Fukui Prefecture, Japan 910-0017, [k]Universidad Iberoamericana, Mexico D.F., Mexico, [l]Iowa State University, Ames, IA 50011, [m]University of Iowa, Iowa City, IA 52242, [n]Kinki University, Higashi-Osaka City, Japan 577-8502, [o]Kansas State University, Manhattan, KS 66506, [p]University of Manchester, Manchester M13 9PL, England, [q]Queen Mary, University of London, London, E1 4NS, England, [r]Muons, Inc., Batavia, IL 60510, [s]Nagasaki Institute of Applied Science, Nagasaki, Japan, [t]National Research Nuclear University, Moscow, Russia, [u]University of Notre Dame,

The flavor-changing neutral current (FCNC) process $b \to s\ell\ell$ occurs in the standard model (SM) only through higher order diagrams where new physics (NP) contributions could arise. Accurate SM predictions make the $b \to s\ell\ell$ phenomenology particularly suited to uncover early indications of NP, especially through observables like the lepton forward-backward asymmetry (A_{FB}) and the differential branching fraction ($\mathcal{B}$) as a function of dilepton mass, extremely sensitive to the interference between the SM and the NP decay amplitudes. The exclusive channels $B^+ \to K^+\mu^+\mu^-$ and $B^0 \to K^*(892)^0\mu^+\mu^-$ have been observed at Belle [1] and BaBar [2], with $\mathcal{O}(10^{-6})$ branching fractions. The decay $B_s^0 \to \phi(1020)\mu^+\mu^-$, however, has not been seen in previous searches by CDF [3] and D0 [4]. Recently, BaBar [5] and Belle [6] measured A_{FB} in the $B^0 \to K^{*0}\ell^+\ell^-$ decay larger than the SM expectation, including data from the small q^2 region ($q^2 \equiv M_{\ell\ell}^2c^2$, where $M_{\ell\ell}$ is the dilepton invariant mass). Belle claims the cumulative difference from the SM prediction corresponds to 2.7 standard deviations.

In this Letter we report an update of our previous analysis [3] of the rare decay modes $B^+ \to K^+\mu^+\mu^-$, $B^0 \to K^{*0}\mu^+\mu^-$, and $B_s^0 \to \phi\mu^+\mu^-$ using an increased data sample of $p\bar{p}$ collisions at a center-of-mass energy of $\sqrt{s} = 1.96$ TeV corresponding to an integrated luminosity of 4.4 fb^{-1}, collected with the CDF II detector between March 2002 and January 2009.

We update the $\mathcal{B}$ measurements and also report the measurement of A_{FB} in the $B^0 \to K^{*0}\mu^+\mu^-$ decay. We reconstruct $B \to h\mu^+\mu^-$ candidates, where B stands for B^+, B^0, or B_s^0, and h stands for K^+, K^{*0}, or ϕ, respectively. Charge-conjugation is implied throughout the Letter. The K^{*0} (ϕ) meson is reconstructed in the decay $K^{*0} \to K^+\pi^-$ ($\phi \to K^+K^-$). We also reconstruct $B \to J/\psi h$ decays as normalization channels in $\mathcal{B}$ measurements, because they have final states identical to those of the signals, resulting in a cancellation of many systematic uncertainties in the ratio of $\mathcal{B}$'s. The relative $\mathcal{B}$'s are described as follows:

$$\frac{\mathcal{B}(B \to h\mu^+\mu^-)}{\mathcal{B}(B \to J/\psi h)} = \frac{N_{h\mu^+\mu^-}}{N_{J/\psi h}} \frac{\varepsilon_{J/\psi h}}{\varepsilon_{h\mu^+\mu^-}} \times \mathcal{B}(J/\psi \to \mu^+\mu^-), \quad (1)$$

where $N_{h\mu^+\mu^-}$ ($N_{J/\psi h}$) is the $B \to h\mu^+\mu^-$ ($B \to J/\psi h$) yield, $\varepsilon_{h\mu^+\mu^-}/\varepsilon_{J/\psi h}$ is the relative reconstruction efficiency that is determined from the Monte Carlo simulation.

The CDF II detector is a multipurpose magnetic spectrometer surrounded by calorimeters and muon detectors. Here we briefly describe the components relevant to this analysis. Charged particles are detected with the tracking system, immersed in a 1.4 T solenoidal magnetic field. A seven-layer silicon tracking system [7], ranging in radius from 1.5 to 22 cm measures the point of origin of charged particle trajectories (tracks). A drift chamber [8] provides 96 measurements per track between radii of 40 and 137 cm, allowing an accurate determination of the charged-particle momentum. The drift chamber also provides identification of high momentum charged particles (1.5σ K–π separation at $p > 2\,\mathrm{GeV}/c$) through the measurement of specific ionization energy loss (dE/dx). A time-of-flight (TOF) detector [9] provides an analogous identification performance in the lower momentum range. Drift chambers [10] are located at the outermost radial extent of the electromagnetic and hadronic calorimeters to detect muons within $|\eta| < 0.6$ and $0.6 < |\eta| < 1.0$, where the pseudorapidity $\eta = -\ln(\tan\theta/2)$ and θ is the track angle measured with respect to the proton beamline.

A sample of dimuon events is selected online using a three-level trigger system. The first trigger level requires the presence of two charged particles with transverse momentum $p_T \geq 1.5$ or $2.0\,\mathrm{GeV}/c$ depending on the trigger condition, matched to track-segments in the muon chambers. The second level requires that the muon candidates have opposite charge with an opening angle in the projection transverse to the beamline less than 120°. At the third level, the trigger selects fully reconstructed events where the muon tracks are reconstructed in the silicon detector and satisfy $L_{xy} > 200$ μm, where L_{xy} is the transverse displacement of their intersection from the beamline.

The offline loose event selection begins by looking for a common vertex of two muons with one (two opposite-charge) reconstructed charged particle(s) to form a $B^+ \to K^+\mu^+\mu^-$ (a $B^0 \to K^{*0}\mu^+\mu^-$ or a $B_s^0 \to \phi\mu^+\mu^-$) candidate. Each muon is required to satisfy the trigger requirements. The probability of the vertex fit χ^2 is required to be greater than 10^{-3}. All charged particle trajectories are required to be associated with hits in the silicon vertex detector and to have $p_T \geq 0.4\,\mathrm{GeV}/c$. In addition, we require $p_T(h) \geq 1.0\,\mathrm{GeV}/c$ and $p_T(B) \geq 4.0\,\mathrm{GeV}/c$. We require that the B candidate's decay is consistent with being displaced from the primary interaction point in the transverse plane by $L_{xy}(B)/\sigma(L_{xy}(B)) \geq 3$, where $L_{xy}(B)$ is the transverse displacement of the reconstructed secondary vertex with respect to the primary interaction point and $\sigma(L_{xy}(B))$ is the estimated uncertainty of $L_{xy}(B)$. We also require that the B candidate comes from the primary vertex by $|d_0(B)| \leq 120$ μm, where $d_0(B)$ is the distance of closest approach of the B trajec-

Notre Dame, IN 46556, [v]Universidad de Oviedo, E-33007 Oviedo, Spain, [w]Texas Tech University, Lubbock, TX 79609, [x]IFIC(CSIC-Universitat de Valencia), 56071 Valencia, Spain, [y]Universidad Tecnica Federico Santa Maria, 110v Valparaiso, Chile, [z]University of Virginia, Charlottesville, VA 22906, [aa]Yarmouk University, Irbid 211-63, Jordan, [ii]On leave from J. Stefan Institute, Ljubljana, Slovenia,

tory to the beamline.

For B^0 (B_s^0) candidates the $K^+\pi^-$ (K^+K^-) mass must lie within 50 (10) MeV/c^2 of the world average K^{*0} (ϕ) mass [11]. The ambiguity of the mass assignment in the $K^{*0} \to K^+\pi^-$ decay is handled by choosing the combination with the $K^+\pi^-$ mass closer to the known K^{*0} mass. This results in the correct mass assignments for about 92% of the decays as determined from the simulation. Particle identification (PID) is performed with the TOF and dE/dx probabilities of the particle hypothesis. We require loose PID for both kaons and pions coming from the K^{*0} meson or ϕ meson to reduce combinatorial background. This removes 15% of the B mass sideband events (defined later) while 99.5% of the signal is retained. We also require a muon likelihood [12] to suppress hadron tracks that produce false trigger muons.

Rare decay candidates with a dimuon mass near the J/ψ (ψ') are rejected: 8.68 $(12.86) < q^2 < 10.09$ (14.18) GeV$^2/c^2$. To eliminate the radiative charmonium decays that escaped rejection above, we remove candidates consistent with originating from a $B \to J/\psi(')h$ decay followed by the decay of the $J/\psi(')$ into two muons and a photon: $|(M(\mu\mu\mathrm{h}) - M_B^{\mathrm{PDG}}) - (M(\mu\mu) - M_{\mathrm{J}/\psi(')}^{\mathrm{PDG}})| < 100\,\mathrm{MeV}/c^2$, where the PDG superscript indicates known experimental averages [11] and $M(\mu\mu) < \mathrm{M}_{\mathrm{J}/\psi(')}^{\mathrm{PDG}}$. We also reject candidates with an opposite-sign hadron-muon combination, which are reconstructed as signal and are assigned the muon mass to both particles, within $40\,\mathrm{MeV}/c^2$ of the J/ψ or ψ' mass. This removes the charmonium decays where one of the muons is misidentified as a hadron. We reject candidates in which two-track (three-track) combinations are compatible within $\pm 25\,\mathrm{MeV}/c^2$ with $D^0 \to K^-\pi^+$ ($D^+ \to K^-\pi^+\pi^+$ or $D_s^+ \to K^+K^-\pi^+$) decays for B^+, B^0, and B_s^0 decays, respectively. This removes $B \to D\pi$ ($D = D^0$, D^+, and D_s^+) decays where two hadrons are misidentified as muons.

The search for the rare decays is performed using a multivariate Artificial Neural Network (NN) classifier. We train the NN on simulated signal and a sample of events representative of the background events under the signal. To simulate the signal we use PYTHIA [13] and EvtGen [14] based on the SM expectation [15]. The background sample is obtained from the sidebands of the B invariant mass distribution, defined as the regions $+5\sigma$ to $+15\sigma$ above the world average B mass, with the B mass width $\sigma = 20\,\mathrm{MeV}/c^2$. We take only the higher mass sideband for the B^+ and B^0 decays, since the lower sideband is significantly populated with physics background from partially reconstructed B meson decays. We use both sidebands for B_s^0 decays. We optimize the NN threshold in order to maximize both the $\mathcal{B}$ and the $\mathrm{A_{FB}}$ significance. For the B^+ and B^0 analysis we optimize the NN threshold by maximizing $N_s/\sqrt{N_s + N_b}$, where N_s is the expected number of signal events, and N_b is the expected background. We determine N_s by Eq. (1) with the world average $\mathcal{B}$, and determine N_b from the number of sideband events scaled to the signal region, which is defined as $\pm 2\sigma$ from the world average B mass. For B_s^0 decays, N_s is taken from a theoretical prediction [16]. We maximize $N_s/(5/2 + \sqrt{N_b})$ [17].

The signal yield is obtained by an unbinned maximum log-likelihood fit to the B candidate invariant mass distribution. The likelihood is constructed from the product of the event-by-event signal and background probability density functions (PDFs) appropriately weighted for signal and background and is given by $\mathcal{L} = \prod(f_{\mathrm{sig}}\mathcal{P}_{\mathrm{sig}} + (1 - f_{\mathrm{sig}})\mathcal{P}_{\mathrm{bg}})$, where f_{sig} is the signal fraction, $\mathcal{P}_{\mathrm{sig}}$ is the signal PDF parametrized with two Gaussian distributions with different means, and $\mathcal{P}_{\mathrm{bg}}$ is the background PDF modeled with a first- or second-order polynomial. The shape variables of the signal PDF are determined from the simulated signal and the B mass resolution is scaled by the ratio of the mass resolution in $J/\psi h$ data and simulation, which ranges from 1.07 to 1.09. The shape variables of the background are determined from sideband data. Fitted parameters are f_{sig}, the mean B mass, and the background shape. The fit range for B^+ and B^0 (B_s^0) decays is from 5.18 (5.00) to $5.70\,\mathrm{GeV}/c^2$, to avoid the region dominated by the physics background.

We consider charmless B decays and the crosstalk among the rare decays as possible sources of backgrounds, which appear predominantly in the signal region. While the contribution from charmless B decays is negligible due to excellent muon identification, we find a sizeable crosstalk between $B^0 \to K^{*0}\mu^+\mu^-$ and $B_s^0 \to \phi\mu^+\mu^-$ contributing approximately 1% of the signal, as estimated from simulation. These contributions, whose fractions are determined by simulation assuming the world average $\mathcal{B}$ and the theoretical prediction [16], are subtracted from the fit results for the signal yields.

From the B mass fits we obtain 120 ± 16, 101 ± 12, and 27 ± 6 signal events for $B^+ \to K^+\mu^+\mu^-$, $B^0 \to K^{*0}\mu^+\mu^-$, and $B_s^0 \to \phi\mu^+\mu^-$, respectively, where the uncertainties include the Poisson term from finite statistics of the whole sample. Figure 1 shows the B mass distributions. The statistical significance is $s \equiv \sqrt{-2\ln(\mathcal{L}_{\mathrm{null}}/\mathcal{L}_{\mathrm{max}})}$, where $\mathcal{L}_{\mathrm{max}}$ is obtained from a fit with the signal fraction free to float and the mean B meson mass fixed to the fitted value in the corresponding control channel, and $\mathcal{L}_{\mathrm{null}}$ is the maximum likelihood obtained from a fit with $f_{\mathrm{sig}} = 0$. We obtain $s = 8.5\sigma$, 9.7σ, and 6.3σ for B^+, B^0, and B_s^0 decays, respectively. This is the first observation of the $B_s^0 \to \phi\mu^+\mu^-$ mode.

We do not apply a NN selection to $J/\psi h$ channels, because these signals are of sufficient size and purity with the loose selection. To obtain the relative efficiency of Eq. (1), the NN cut efficiency of the loosely selected events is considered in addition to the relative efficiency of the loose selection.

The dominant sources of systematic uncertainty on the

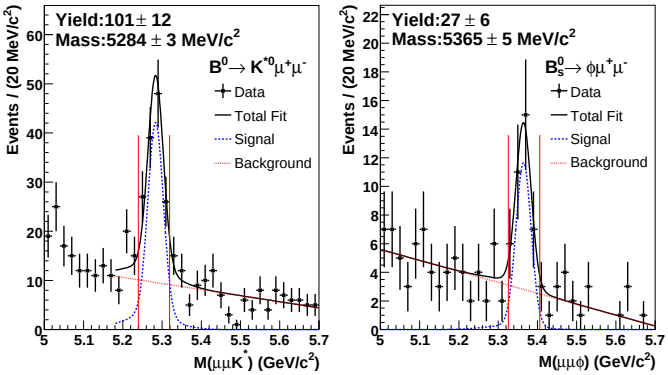

FIG. 1: Mass of $B^0 \to K^{*0}\mu^+\mu^-$ and $B_s^0 \to \phi\mu^+\mu^-$ candidates with fit results overlaid. The vertical lines show the signal region.

$\mathcal{B}$ measurements are the discrepancy of the NN cut efficiency between data and simulation, background PDF parameterization, acceptance differences due to form factor models used in the simulation. These have systematic effects up to 5% of the measured $\mathcal{B}$. For the absolute $\mathcal{B}$ measurements we assign the uncertainties of the world average $\mathcal{B}(B \to J/\psi h)$ [11].

Results of the relative $\mathcal{B}$ (Eq. (1)) measurements are listed in Table I. We also show the absolute $\mathcal{B}$ which is obtained by replacing the control channel's $\mathcal{B}$ with the corresponding world average [11] value. These numbers are consistent with our previous results [3], other B-factory measurements [6, 18], and the theoretical expectations [16].

TABLE I: Measured branching fractions of rare modes. First (second) uncertainty is statistical (systematic).

Mode	Relative $\mathcal{B}(10^{-3})$	Absolute $\mathcal{B}(10^{-6})$
$B^+ \to K^+\mu^+\mu^-$	$0.38 \pm 0.05 \pm 0.02$	$0.38 \pm 0.05 \pm 0.03$
$B^0 \to K^{*0}\mu^+\mu^-$	$0.80 \pm 0.10 \pm 0.06$	$1.06 \pm 0.14 \pm 0.09$
$B_s^0 \to \phi\mu^+\mu^-$	$1.11 \pm 0.25 \pm 0.09$	$1.44 \pm 0.33 \pm 0.46$

We also measure the differential $\mathcal{B}$s with respect to the dimuon mass. Events in the signal mass region are grouped into five or six independent q^2 bins. Figure 2 (a, b) shows the differential $\mathcal{B}$ for $B^+ \to K^+\mu^+\mu^-$ and $B^0 \to K^{*0}\mu^+\mu^-$.

The A_{FB} and the K^{*0} longitudinal polarization (F_L) are extracted by an unbinned likelihood fit to the $\cos\theta_\mu$ and $\cos\theta_K$ distributions, respectively, where θ_μ is the helicity angle between the μ^+ (μ^-) direction and the direction opposite to the B ($\overline{B}$) meson in the dimuon rest-frame, and θ_K is the angle between the kaon direction and the direction opposite to the B meson in the K^{*0} rest frame. The differential decay rates [19] are sensitive to $\cos\theta_K$ and $\cos\theta_\mu$ through the angular distributions given by $\frac{3}{2}F_L\cos^2\theta_K + \frac{3}{4}(1-F_L)(1-\cos^2\theta_K)$ for the $\cos\theta_K$ and $\frac{3}{4}F_L(1-\cos^2\theta_\mu) + \frac{3}{8}(1-F_L)(1+\cos^2\theta_\mu) + A_{FB}\cos\theta_\mu$ for the $\cos\theta_\mu$ distribution. The PDFs include the decay angular distributions and the likelihood fits are, thus, sensitive to the variables in the decay distributions. We measure F_L and A_{FB} for $B^0 \to K^{*0}\mu^+\mu^-$ and also A_{FB} for $B^+ \to K^+\mu^+\mu^-$. Angular acceptances of $\cos\theta_K$ and $\cos\theta_\mu$ are considered as histograms obtained from simulated signal samples assuming unpolarized decays. The contribution from decays with K-π swapped K^{*0} mesons distorts the signal distribution and swaps the sign of $\cos\theta_\mu$. This effect is considered by adding an additional signal-like term to the likelihood function. The contribution from decays with non-resonant K-π is considered to be small [19] and neglected in the fit. For the B^+ decay, we set $F_L = 1$ and consider no scalar term [20].

The combinatorial background PDF shape is taken from the B mass upper sideband that is used for the NN training. The sideband data are divided into five or six q^2 bins and the angular variables $\cos\theta_K$ and $\cos\theta_\mu$ are described as histograms. In the fit to $\cos\theta_K$ ($\cos\theta_\mu$) distribution, the only free parameter is F_L (A_{FB}).

The dominant sources of systematic uncertainty on the measurement of F_L in the B^0 decay are due to the uncertainty of the signal fraction, angular acceptance, and fit bias near the physical boundary. For the measurement of A_{FB} in the B^0 decay mode, the dominant systematic uncertainty arises from the F_L fit. The systematic uncertainty on the A_{FB} measurement in the B^+ decay is dominated by the signal fraction uncertainty, angular background shape and angular acceptance. The total systematic uncertainties range in 0.02–0.08, 0.05–0.25, and 0.02–0.08 for F_L in B^0 and A_{FB} in B^0 and A_{FB} in B^+, respectively.

The results of the fit in six q^2 bins are shown in Fig. 2 (c, d) and summarized in Table II. Results in the range $0 \le q^2 < 4.3\,\mathrm{GeV}^2/c^2$ and $1 \le q^2 < 6\,\mathrm{GeV}^2/c^2$ are also included.

In summary, we have updated our previous analysis of FCNC decays $b \to s\mu\mu$ using data corresponding to an integrated luminosity of 4.4 fb^{-1}. We report the first observation of the $B_s^0 \to \phi\mu^+\mu^-$, the most rare B_s^0 decay observed to date, and measure the total $\mathcal{B}$. We measure the total $\mathcal{B}$, differential $\mathcal{B}$, F_L, and A_{FB} of the $B^+ \to K^+\mu^+\mu^-$ and $B^0 \to K^{*0}\mu^+\mu^-$, with respect to q^2. These are consistent and competitive with the other current best results. At present there is no evidence of discrepancy from the SM prediction.

We thank the Fermilab staff and the technical staffs of the participating institutions for their vital contributions. This work was supported by the U.S. Department of Energy and National Science Foundation; the Italian Istituto Nazionale di Fisica Nucleare; the Ministry of Education, Culture, Sports, Science and Technology of Japan; the Natural Sciences and Engineering Research Council of Canada; the National Science Council of the

TABLE II: Summary of $B^0 \to K^{*0}\mu^+\mu^-$ and $B^+ \to K^+\mu^+\mu^-$ fit results. Maximum q^2 is 19.30 (23.00) GeV$^2/c^2$ for B^0 (B^+).

q^2 (GeV$^2/c^2$)	$\mathcal{B}(10^{-7})$	F_L	A_{FB}	$\mathcal{B}(10^{-7})$	A_{FB}
	$B^0 \to K^{*0}\mu^+\mu^-$			$B^+ \to K^+\mu^+\mu^-$	
$[0.00, 2.00)$	$0.98 \pm 0.40 \pm 0.09$	$0.53^{+0.32}_{-0.34} \pm 0.07$	$0.13^{+1.65}_{-0.75} \pm 0.25$	$0.38 \pm 0.16 \pm 0.03$	$-0.15^{+0.46}_{-0.39} \pm 0.08$
$[2.00, 4.30)$	$1.00 \pm 0.38 \pm 0.09$	$0.40^{+0.32}_{-0.33} \pm 0.08$	$0.19^{+0.40}_{-0.41} \pm 0.14$	$0.58 \pm 0.19 \pm 0.04$	$0.72^{+0.40}_{-0.35} \pm 0.07$
$[4.30, 8.68)$	$1.69 \pm 0.57 \pm 0.15$	$0.82^{+0.19}_{-0.23} \pm 0.07$	$-0.06^{+0.30}_{-0.28} \pm 0.05$	$0.93 \pm 0.25 \pm 0.06$	$-0.20^{+0.17}_{-0.28} \pm 0.03$
$[10.09, 12.86)$	$1.97 \pm 0.47 \pm 0.17$	$0.31^{+0.19}_{-0.18} \pm 0.02$	$0.66^{+0.23}_{-0.20} \pm 0.07$	$0.72 \pm 0.17 \pm 0.05$	$-0.10^{+0.17}_{-0.15} \pm 0.07$
$[14.18, 16.00)$	$1.51 \pm 0.36 \pm 0.13$	$0.55^{+0.17}_{-0.18} \pm 0.02$	$0.42^{+0.16}_{-0.16} \pm 0.09$	$0.38 \pm 0.12 \pm 0.03$	$0.03^{+0.49}_{-0.16} \pm 0.04$
$[16.00, 19.30(23.00))$	$1.35 \pm 0.37 \pm 0.12$	$0.09^{+0.18}_{-0.14} \pm 0.03$	$0.70^{+0.16}_{-0.25} \pm 0.10$	$0.35 \pm 0.13 \pm 0.02$	$0.07^{+0.30}_{-0.23} \pm 0.02$
$[0.00, 4.30)$	$1.98 \pm 0.55 \pm 0.18$	$0.47^{+0.23}_{-0.24} \pm 0.03$	$0.21^{+0.31}_{-0.33} \pm 0.05$	$0.96 \pm 0.25 \pm 0.06$	$0.36^{+0.24}_{-0.26} \pm 0.06$
$[1.00, 6.00)$	$1.60 \pm 0.54 \pm 0.14$	$0.50^{+0.27}_{-0.30} \pm 0.03$	$0.43^{+0.36}_{-0.37} \pm 0.06$	$1.01 \pm 0.26 \pm 0.07$	$0.08^{+0.27}_{-0.22} \pm 0.07$

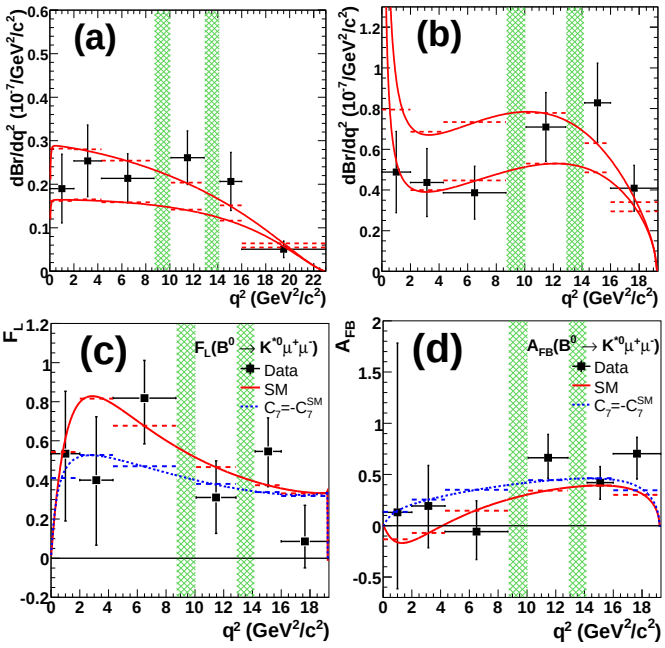

FIG. 2: Differential $\mathcal{B}$ of $B^+ \to K^+\mu^+\mu^-$ (a) and differential $\mathcal{B}$ (b), longitudinal K^{*0} polarization (c), and forward-backward asymmetry (d) of $B^0 \to K^{*0}\mu^+\mu^-$, as a function of squared dimuon mass. Points are the fit result. The solid curve is the SM expectation [15], which use maximum- and minimum- allowed form factors on differential $\mathcal{B}$ plots. The dotted curve is the $C_7 = -C_7^{\rm eff}_{\rm SM}$ expectation, where C_7 is one of the Wilson coefficients [21]. The dashed line is the averaged expectation in each squared dimuon mass bin and hatched regions are charmonium veto regions.

Republic of China; the Swiss National Science Foundation; the A.P. Sloan Foundation; the Bundesministerium für Bildung und Forschung, Germany; the World Class University Program, the National Research Foundation of Korea; the Science and Technology Facilities Council and the Royal Society, UK; the Institut National de Physique Nucleaire et Physique des Particules/CNRS; the Russian Foundation for Basic Research; the Ministerio de Ciencia e Innovación, and Programa Consolider-Ingenio 2010, Spain; the Slovak R&D Agency; and the Academy of Finland.

[1] K. Abe *et al.* (BELLE Collaboration), Phys. Rev. Lett. **88**, 021801 (2002); A. Ishikawa *et al.* (BELLE Collaboration), Phys. Rev. Lett. **91**, 261601 (2003).
[2] B. Aubert *et al.* (BABAR Collaboration), Phys. Rev. Lett. **91**, 221802 (2003).
[3] T. Aaltonen *at al.* (CDF Collaboration), Phys. Rev. D**79**, 011104 (2009).
[4] V. M. Abazov *et al.* (D0 Collaboration), Phys. Rev. D**74**, 031107 (2006).
[5] B. Aubert *et al.* (BABAR Collaboration), Phys. Rev. D**79**, 031102 (2009).
[6] J. T. Wei *et al.* (BELLE Collaboration), Phys. Rev. Lett. **103**, 171801 (2009).
[7] A. Sill (CDF Collaboration), Nucl. Instrum. Meth. A**447**, 1 (2000).
[8] A. A. Affolder *et al.* (CDF Collaboration), Nucl. Instrum. Meth. A**526**, 249 (2004).
[9] D. Acosta *et al.* (CDF-II Collaboration), Nucl. Instrum. Meth. A**518**, 605 (2004).
[10] G. Ascoli *et al.*, Nucl. Instrum. Meth. A**268**, 33 (1988); T. Dorigo (CDF Collaboration), Nucl. Instrum. Meth. A**461**, 560 (2001).
[11] K. Nakamura *et al.* (Particle Data Group), J. Phys. G**37**, 075021 (2010).
[12] T. Aaltonen *et al.* (CDF Collaboration), Phys. Rev. Lett. **100**, 101802 (2008).
[13] T. Sjöstrand *et al.*, Comput. Phys. Commun. **135**, 238 (2001).
[14] D. J. Lange, Nucl. Instrum. Meth. A**462**, 152 (2001).
[15] A. Ali, P. Ball, L. T. Handoko, and G. Hiller, Phys. Rev. D**61**, 074024 (2000).
[16] C. Q. Geng and C. C. Liu, J. Phys. G**29**, 1103 (2003).
[17] G. Punzi, arXiv:physics/0401045.
[18] B. Aubert *et al.* (BABAR Collaboration), Phys. Rev. Lett. **102**, 091803 (2009).
[19] F. Kruger and J. Matias, Phys. Rev. D**71**, 094009 (2005).
[20] C. Bobeth, G. Hiller, and G. Piranishvili, J. High Energy Phys. 12 (2007) 040.
[21] K. G. Wilson, Phys. Rev. **179**, 1499 (1969).